

Force transfer mechanism in positive moment continuity details for prestressed concrete girder bridges

Tanvir Hossain^{1a} and Ayman M. Okeil^{*2}

¹*SBM Offshore, Houston, TX, USA*

²*Department of Civil and Environmental Engineering, Louisiana State University, Baton Rouge, LA 70803, USA*

(Received December 21, 2012, Revised May 10, 2014, Accepted May 26, 2014)

Abstract. The force transfer mechanism in positive moment continuity details for prestressed concrete girder bridges is investigated in this paper using a three-dimensional detailed finite element model. Positive moment reinforcement in the form of hairpin bars as recommended by the National Cooperative Highway Research Program Report No 519 is incorporated in the model. The cold construction joint that develops at the interface between girder ends and continuity diaphragms is also simulated via contact elements. The model is then subjected to the positive moment and corresponding shear forces that would develop over the service life of the bridge. The stress distribution in the continuity diaphragm and the axial force distribution in the hairpin bars are presented. It was found that due to the asymmetric configuration of the hairpin bars, asymmetric stress distribution develops at the continuity diaphragm, which can be exacerbated by other asymmetric factors such as skewed bridge configurations. It was also observed that when the joint is subjected to a positive moment, the tensile force is transferred from the girder end to the continuity diaphragm only through the hairpin bars due to the lack of contact between the both members at the construction joint. As a result, the stress distribution at girder ends was found to be concentrated around the hairpin bars influence area, rather than be resisted by the entire girder composite section. Finally, the results are used to develop an approach for estimating the cracking moment capacity at girder ends based on a proposed effective moment of inertia.

Keywords: continuity detail; positive moment; diaphragm; axial force; finite element

1. Introduction

Continuous prestressed concrete girder bridges offer many advantages over simple span bridges. Continuous bridges eliminate the joints over intermediate piers, which in addition to being weak structural links, they also eliminate the possibility of water leaks over the piers which is detrimental to reinforced concrete structures, especially when deicing agents are used. As a result of eliminating the problems associated with joints, maintenance costs are drastically reduced and the riding quality improves. Structurally, live load positive moments at the midspan of a continuous bridge are in general less than those that develop in a simply supported bridge (Wang *et al.* 2011).

*Corresponding author, Associate Professor, E-mail: aokeil@lsu.edu

^aStructural Engineer, E-mail: Tanvir.Hossain@sbmoffshore.com

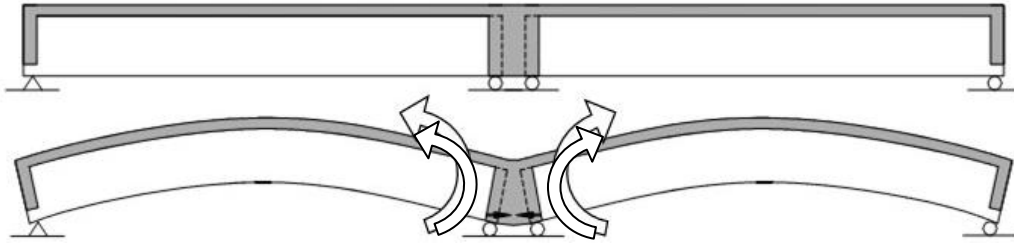


Fig. 1 Positive moment development at the diaphragm

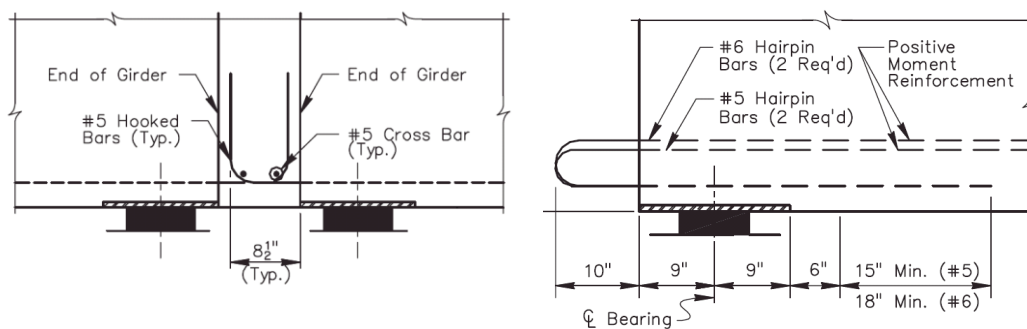


Fig. 2 Positive moment reinforcement alternatives.

Consequently, more economic designs can be achieved as the span lengths for the same sections of girders may be increased; resulting in fewer piers or fewer prestressing strands if the span lengths are kept the same as those of simple span construction. Furthermore, continuity offers an important structural benefit by enhancing the redundancy of the superstructure, which is a desirable property in any structural system, especially for those in seismically active zone.

Simple span girder bridges are made continuous in different ways. One of which is to cast a continuous deck over the girders while keeping the space in between the girder ends free to allow relative movement between bottoms of girder ends. Extra reinforcement in the deck provides resistance to negative moments that develop over piers due to gravity loads. This approach results in partial continuity of the system as compared to a fully continuous system (Caner and Zia 1998; Caner *et al.* 2002; Okeil and El-Safty 2005; El-Safty and Okeil 2008). Alternatively, simple span girders can be converted into continuous structures by pouring concrete in between the girders' ends over the piers in the form of a continuity diaphragm. This design alternative results in fully continuous structures when designed adequately. The state of the art of continuous bridge construction can be found in Hastak *et al.* (2003).

Prestressed concrete girders camber up as a result of applying the prestressing forces where the tension is to be expected; i.e. below the neutral axis at midspans. This instantaneous camber keeps increasing through the life of the prestressed girder due to creep of concrete (Sousa *et al.* 2012). When the girders are placed as a simple span on the piers, girder ends rotate as shown in Fig. 1. If continuity is established between the girders by pouring a continuity diaphragm, girder end rotations are restrained, which leads to the development of tensile forces at the bottom of diaphragm. If this tensile force exceeds the rupture strength of the diaphragm concrete, the bottom of the diaphragm cracks and allows the girder ends to rotate. Thus, continuity is lost and the girder

behaves as a simple span or as a partially continuous system as described earlier. Positive moment reinforcement is, therefore, provided at the bottom of the diaphragm to resist the tensile forces that develop from girder's camber due to creep and other loads such as temperature gradients and some special live load position (Newhouse *et al.* 2008). The additional positive moment reinforcement can be provided in the form of extra bars extruding out from the bottom flange of the girders. Alternatively, the prestressing strands can be extended out from the bottom flange and bent upward into the diaphragm.

Several researchers looked into the advantages of each alternative, and design methods have been proposed (Oesterle *et al.* 1989; Peterman and Ramirez 1998; Mirmiran *et al.* 2001). Recently, the National Cooperative Highway Research Program (NCHRP) sponsored Project 12-53 on positive moment continuity details for continuous prestressed concrete girder bridges. The findings of the project were published in NCHRP Report 519 (Miller *et al.* 2004). The report covered the two aforementioned alternatives for the detailing: (1) extending the prestressing strands from the girders' bottom flanges into the continuity diaphragm and (2) providing additional 90°-hook or 180°-hook reinforcing bars (a.k.a. hairpin bars if both ends of the bar are developed in the girder) at the bottom flange that extend into the diaphragm.

Fig. 2 shows both alternatives covered in NCHRP Report 519. The number of strands and length of the embedment of the strand into the continuity diaphragm can be found from the equations developed by Salmons and May (1974). The design recommendations resulting from NCHRP Project 12-53 were adopted into provisions in AASHTO LRFD Bridge Design Specifications (2010) to assist designers in detailing the positive moment reinforcement. One of the concern of this type of connection is that, congestion in the diaphragm area might reduce the capacity of the connections due to the lack of interaction between bar and concrete. Another concern for bent bar connection is that bars must be placed asymmetrically with respect to the cross section to avoid space conflict between bars extending from opposite girders. This asymmetrical layout may lead to nonuniform stress distribution, which, if exacerbated by other factors such as a skewed bridge layout, may lead to higher than anticipated stresses, thus, increasing the chances of cracking. The 180°-hook bar was recommended over 90°-hook bent bar connection because of the difficulties associated with placing the 90°-hook bent bar because of their interference with the formwork. Therefore, 180° bent bars were recommended as a possible alternative in the NCHRP 519 Report (Miller *et al.* 2004).

A recently completed project in Southern Louisiana was bid as a design build project. The John James Audubon Project creates a new transportation artery across the Mississippi River between the cities of New Roads and Saint Francisville. In addition to the main cable stayed bridge that crosses the Mississippi River, seven approach bridges had to be constructed. The designer of the project adopted one of the recommended continuity details (180°-hook hairpin bars) in many of the prestressed concrete girder spans. This detail is different than the standard detail in the Louisiana Department of Transportation and Development (LA-DOTD) Bridge Design Manual (BDM). In Louisiana, continuity diaphragms are detailed with no positive moment reinforcement, and to minimize restraint to girder end movement, a bond breaker is applied on the girder ends. Thus, girder bottoms are allowed to move independently from the diaphragm as well as with respect to each other. Therefore, it was deemed necessary to evaluate the performance of the new detail. The LA-DOTD Bridge Design Section chose a three span continuous segment of Bridge #2 that was built with Bulb-T girders made continuous using the new detail and was skewed to accommodate an existing railroad. The attributes of this segment; i.e. Bulb-T girders and skew layout, were not covered in the NCHRP 12-53 Project. A research project was initiated with the objective of

understanding the behavior of bridges employing the new continuity detail under time-dependent effects as well as under live loads. A structural health monitoring approach was adopted for the task. Two years of monitoring data were collected from a 96-channel monitoring system to evaluate the time dependent load effects (Okeil *et al.* 2013), and a static live load test was conducted (Hossain *et al.* 2013b). Several three-dimensional (3D) finite element (FE) models were developed for the study. The first FE model is for the complete 3-span monitored bridge segment, which was used to evaluate the global performance of the bridge. An FE line model of the bridge was developed to investigate the performance of the continuity diaphragm due to time dependent loading as well as temperature gradient. A third FE model that focuses explicitly on the continuity joint was also developed. Findings from this study were published in a recent report (Okeil *et al.* 2011).

One of the observations resulting from this main study is that bottom flanges at girder ends are susceptible to cracking. It was hypothesized that even though the positive moments that developed due to time-dependent effects are not large, they are still capable of causing cracking because of the stress concentrations at the joint. The stress concentration stems from the fact that there is a cold joint between the precast girder end and the cast-in-place continuity diaphragm, through which the positive moment reinforcement passes. This means that all of the tension caused by the positive moment will be resisted by the reinforcement, which implies that the cold joint serves as a man-made crack. This behavior renders design calculations that rely on the gross cross-sectional properties in the vicinity of the joint unconservative.

This paper describes presents three dimensional (3-D) finite element (FE) detailed joint model, which takes into account the gradual increase in prestressing force along the transfer length, the existence of cold joints between the cast in place concrete and the precast concrete, and the actual 180°-hook hairpin bar configuration. The objective of this detailed model was to investigate explore the local behavior at the girder ends and diaphragm under service load condition. The behavior of the continuity detail at the interface between the continuity diaphragm and girder ends under service load condition is investigated in this study. The force transfer mechanism between the girder end and continuity diaphragm is also investigated. Using results from the model, an effective moment of inertia of the composite section to resists the load at the diaphragm and at girder ends is proposed.

2. Finite element modeling

Accurate modeling of the local behavior of the continuity detail calls for incorporating several nonlinear features. For example, incorporating the nonlinear material behavior is essential for understanding the ultimate behavior (Shayanfar and Safiey 2008; Kim *et al.* 2012; Lee *et al.* 2014). Geometric nonlinearities affect the structural behavior in two ways. First, the stiffness of structural members may be affected by large deformations, which is an important modeling aspect for slender and thin-walled structural members. Joints like the continuity detail are affected by another form of geometric nonlinearity due to the discontinuity between adjacent surfaces as they separate from each other without resistance when subjected to tensile forces, while still being capable of resisting large compressive forces in case of moment reversal from positive to negative. In the current study, the goal was to investigate the long-term behavior of the continuity detail under service conditions. Over time, prestressed concrete girder bridges are subjected to straining actions caused by time dependent effects such as creep, shrinkage, and temperature gradients. The

Table 1 Concrete properties

Property	Deck Diaphragm	Girder
Compressive strength (psi)	6500	11500
Modulus of elasticity (psi)	4595486	6112569
Poisson's ratio	0.20	0.20
Unit weight (pcf)	150	150

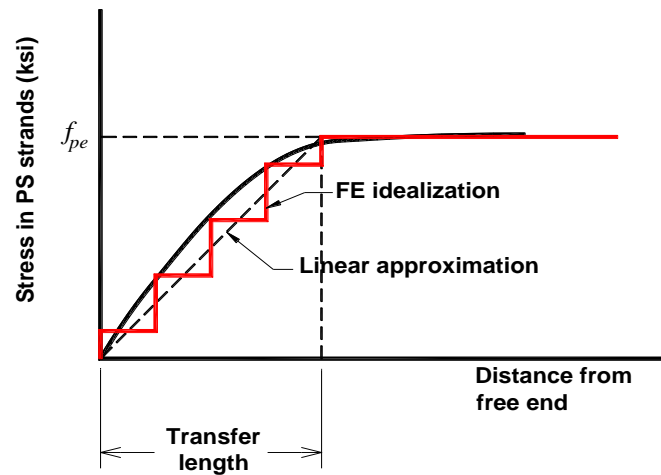


Fig. 3 Finite element idealization of transfer length for prestressing strands

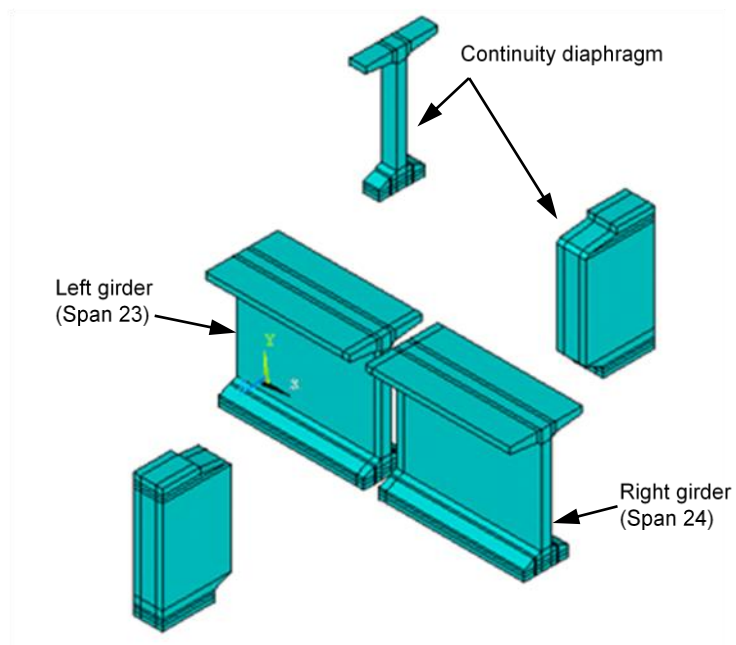


Fig. 4 Construction sequence idealization in finite element modeling (deck not shown for clarity)

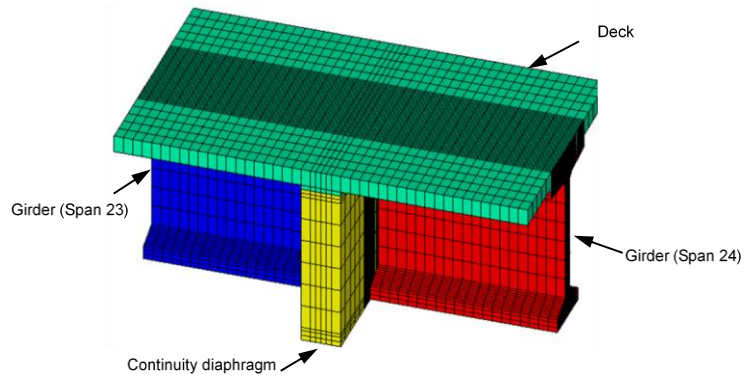
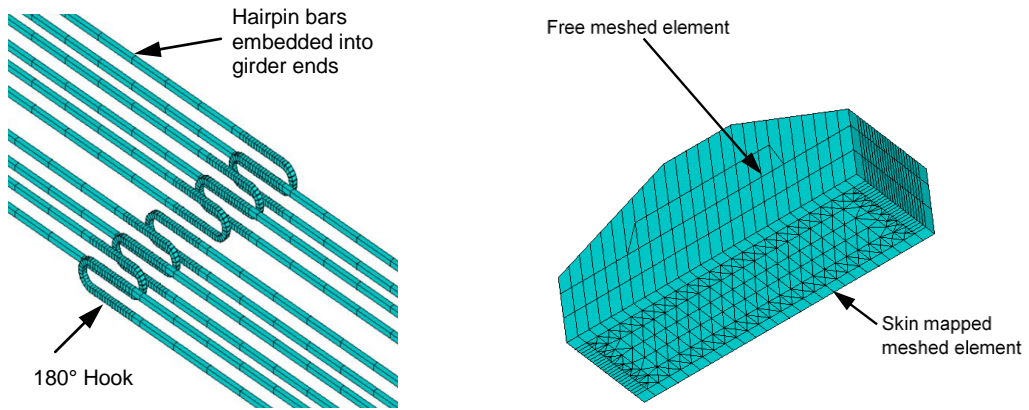
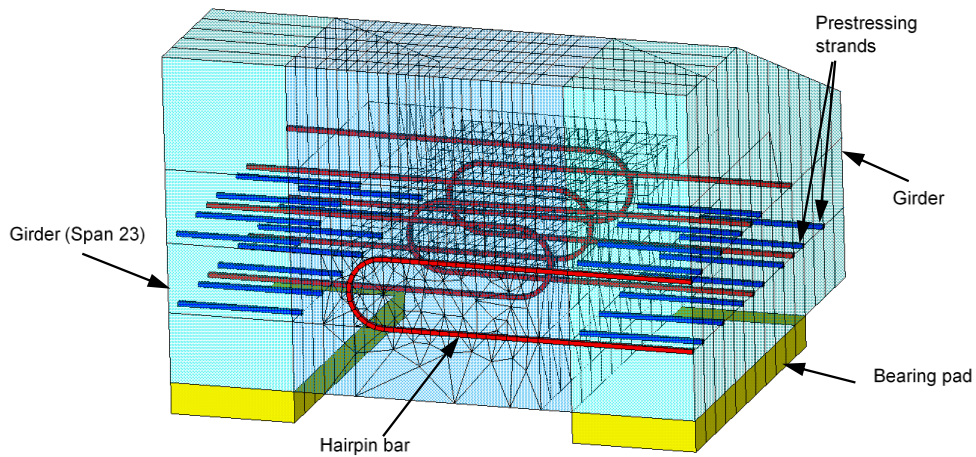


Fig. 5 Elements of the detailed joint model (a coarser mesh is shown here for clarity)



(a) 180° Hairpin bars

(b) Free and mapped mesh regions



(c) Free and mapped mesh (half view)

Fig. 6 Meshing of hairpin bars and bottom of continuity diaphragm

magnitude of the straining actions may be large, however, not to the extent to cause bridge failures. The temperature gradient effect generates a positive continuity moment equal to about 50% of the cracking moment, M_{cr} , according to a study by the authors (Hossain *et al.* 2012). AASHTO-LRFD (2010) calls for limiting the positive moments acting on the continuity detail to be less than $1.2M_{cr}$. As such, large straining actions that can cause the materials to behave at high levels of nonlinearity are not to be expected within the scope of this study. Furthermore, prestressed concrete girders are optimized to eliminate their susceptibility to local buckling and slippage between the positive moment reinforcement and the surrounding concrete is not a factor under service conditions (Shang *et al.* 2010). Hence, it was deemed appropriate to investigate the force transfer mechanism in the continuity detail by developing a detailed 3-D finite element model of the continuity detail without accounting for the material and the geometric nonlinearities. In this study, the main source of nonlinearity that affects the behavior of the continuity detail under service conditions; i.e., cracking is not supposed to take place, is the geometric discontinuity between adjacent surfaces as a result of the cold joint between the precast girders and the cast-in-place diaphragm.

The commercial finite element software package ANSYS (ANSYS 2008) was used to develop the model for investigating the behavior of the continuity detail joint. ANSYS offers a variety of element types that are suitable for building a model capable of capturing the force transfer mechanism in the continuity detail. Element SOLID65, which is an eight node 3-D solid element with six translational degrees of freedom at each node, was used to model the concrete. SOLID65 is capable of modeling cracking and crushing of concrete, which may be needed if further development of the model will be needed in future studies. More importantly, SOLID65 has birth and death features, which is particularly helpful in modeling construction sequence. The input data for concrete material properties include the ultimate uniaxial compressive strength, elastic modulus, density, and Poisson's ratio which are given in Table 1. These values were obtained from construction documents for the analyzed bridge. The prestressing strands were modeled using the LINK8 element, which is a two-noded 3-D spar element with three translational degrees of freedom at each node. Prestressing is applied in the link elements as an initial strain. The initial strain value was determined from the prestressing forces obtained from the fabrication sheets. Since the joint model in this study was intended to investigate the load transfer mechanism at the service load condition, the effective prestress was used in the analysis including the effect of the transfer length. Transfer of the prestressing forces from the strands to the surrounding concrete depends on the transfer length which can be calculated from Eq. (1) (Nawy 2000).

$$l_t = \frac{f_{pe}}{3000} d_b \quad (1)$$

where, f_{pe} is the effective prestress after losses (psi), and d_b is the nominal diameter of prestressing strand (in). The prestressing force in any pretensioned strand starts from zero at the girder end and attains full prestressing level at the transfer length. The increase is nonlinear as can be seen in Fig. 3, however, Eq. (1) simplifies it conservatively with a linear approximation. In the finite element model, the initial strain in LINK8 elements modeling the prestressing strands were changed in the first four elements as illustrated in Fig. 3 to model the actual stresses in the transfer length region. This gradual increase in stress (simulated as an initial strain) is idealized as a step function as shown. Prestressing was assumed to be fully effective at the fifth element from the girder ends which corresponds to a length equal to the transfer length. The hairpin bars were also modeled with LINK8 elements, however, no initial strains were input for these non-prestressed

bars.

In the actual construction sequence, girders were cast at a casting yard where they were stored until cured. After some designated time these girders were then transported to the site and erected on the piers as simple spans. Continuity was then established by pouring the deck and diaphragm concrete. The bridge system starts behaving as a continuous system when the deck and diaphragm concrete harden. Because of this construction sequence, the deck/diaphragm and the girder are not monolithically cast, and a cold joint forms at the interface between the girder ends and diaphragm. Subjecting this interface to compressive stresses (e.g. caused by negative moments) results in that both the girder end and the diaphragm become in full contact and the forces are transferred directly between the concretes of both members. Conversely, when the continuity diaphragm is subjected to tensile forces (e.g. caused by positive moments), the weak bond at the cold joint interface breaks easily and the tension force only transferred from the bottom girder flange to the continuity diaphragm through the hairpin bars. This behavior was simulated using contact elements between the girder ends and the continuity diaphragm. CONTA178 element from the ANSYS library was adopted for this purpose in the current study. CONTA178 represents the contact and sliding between two nodes in any types of ANSYS elements. The contact element is defined by two nodes; one on each of the two touching surfaces, with three translational degrees of freedom at each node. In the developed model, two coincident nodes; i.e., nodes with identical coordinates, were created and connected using the contact element. As such, the contact element has a zero size and its sole purpose is to simulate the separation between the girder ends and the continuity diaphragm. This was achieved by modeling the girders, deck, haunch and the continuity diaphragm separately. The different parts that can be seen in Fig. 4 were then combined together in the final model. In this way, two identical nodes were created along the interfacing surfaces. CONTA178 elements were then added between the identical node pairs. Identical nodes other than those at the girder end and the continuity diaphragm interface were merged together, implying monolithic construction between these parts (e.g. deck and continuity diaphragm).

As will be discussed later, the model was loaded at the ends of the considered portions of the girder with loads equivalent to those developing in the full structure. Therefore, the girder portion considered in the model was taken equal to 7 feet longitudinally to address the Saint-Venant's principle which states that the difference between the effects of two different but statically equivalent loads becomes very small at sufficiently large distances from the load (Timoshenko and Gere 2009). The considered girder portion was taken as 84 inches, which is slightly larger than the total combined height of the composite section including 72 inches for the Bulb-T girder height, 2 inches for the haunch and 7.5 inches for deck thickness totaling 81.5 inches. Girder ends at the continuity diaphragm were placed on the bearing pads whose dimensions and properties were taken from the design plans. SOLID45 elements were used to model the bearing pads. The shear modulus for the bearing pads was taken equal to 95 psi, which is the lower bound value of the AASHTO LRFD Specification (2010). The final mesh of the model is shown in Fig. 5.

One of the most difficult challenges of this study is to model the actual geometry of the 180°-hook hairpin bars. The hairpin bars were extended from the bottom flange of the girder ends and then took the form of standard AASHTO specified 180° hook, which was embedded 8 inches into the continuity diaphragm. Five hairpin bars were extended from each of the adjacent girder ends. These ten hairpin bars were staggered in a way to allow 8 inches of embedment into the continuity diaphragm without creating any conflicts between hairpin bars extending from both girder ends. Modeling the exact geometry of the 180°-hook is extremely important in understanding the local behavior of the continuity diaphragm. Simplification of the hook using square-shaped bar

geometries or curtailing it in any way other than the actual geometry defeats the purpose from building this model. Therefore, a cylindrical shaped volume was defined and overlapped with the rectangular shaped volume. In this way 180° lines were created that were aligned with actual locations of the hairpin bars. These lines were later meshed with elements whose attributes were those for the nonprestressed steel bars as can be seen in Fig. 6a. The different parts of the model within the continuity diaphragm were meshed after the outlines of the hairpin bars were defined. Fully controlled mapped meshing was not possible for all parts because of the complexity of the generated geometries, especially the cylindrical ones. Therefore, free meshing had to be relied on in some parts. To control the transition (zooming) of the mesh between the free meshed and map meshed portions, a substructure of the model representing the small portion of the continuity diaphragm identified by the projection of the bottom flange of the girder was generated. A skin layer of volumes was defined around the free mesh volumes for which the elements were sized to match the mapped mesh elements (see Fig. 6b). Thus, the mapped and free mesh portions of the model shared the same nodes at their junction in the final model. Fig. 6c shows the meshing of a portion of the continuity diaphragm between the girder bottom flanges where the hairpin bars, the prestressing strands, the free and the mapped meshed volumes. The FE model was built using 47,777 elements, 41,592 nodes, and 123,528 degrees of freedom.

3. Loading

The objective of the present study is to investigate the force transfer mechanism between the girder ends of a continuous bridge through the continuity diaphragm with the help of 180° -hook hairpin bars. As mentioned earlier, the focus of the investigation is on the behavior of the continuity detail under positive moments for which the hairpin bars are added to resist the tensile forces resulting from the positive moments. Positive moments may be caused by time-dependent effects such as creep and shrinkage. It may also develop due to temperature gradients and some live load positions. Applying arbitrary positive moments at the girder ends is an option for performing the desired investigation. However, the results may not represent the actual behavior of the continuity detail since these moments may be different than the positive moment acting on the continuity detail. Therefore, straining actions were extracted from a 3-D FE girder line model that was developed to estimate the creep induced moments in the center girder of the monitored bridge segment (Hossain *et al.* 2013a). The FE line model was first calibrated using field monitoring data, and then was used to analyze a representative girder for 75 years, which is the typical service life expected from newly designed bridges. In the line model, positive moments start developing after continuity is established by pouring the continuity diaphragm, which is accounted for by modeling the construction sequence. The bending moment and shear force acting on two sections at a distance equal to 84 inches from the girder ends were obtained by integrating internal stresses caused by creep after 75 years of time. The distance where the moment and shear are obtained was chosen to be the same as the girder length included in the joint model developed in the current study which is equal to the sections height to eliminate the St. Venant effect. The bending moment was the result of integrating the normal stress with respect to the neutral axis of the composite section, which is located at 54.57 inches from the girder's soffit, while the corresponding shear force acting on the same section was obtained by integrating the shear stresses. The self weight of the elements included in the model was included directly as a gravity load. In addition to the creep

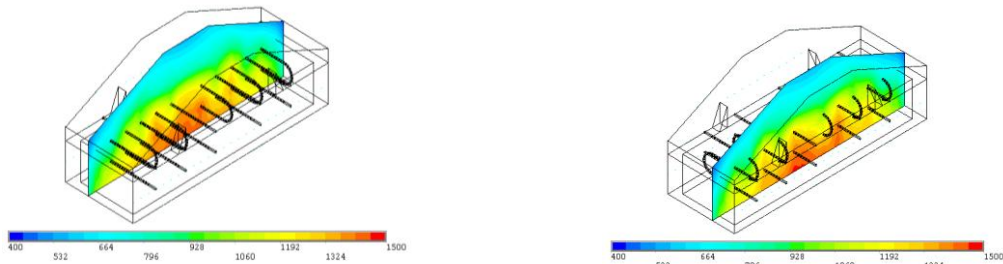
induced equivalent loads and the self weight of the members, the model also included the effect of the prestressing forces from the strands including the transfer length effect as described earlier.

4. Results

The FE model generates a large amount of information that can be used in several types of behavioral assessments. In this section, the focus will be on three aspects of the behavior; namely, asymmetric stress distribution in the continuity diaphragm, hairpin bar contribution, and stress concentrations at girder ends

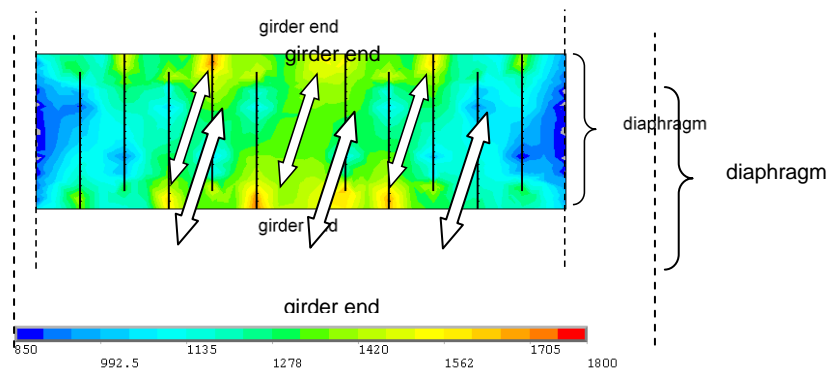
4.1 Asymmetric stress distribution

The stress distribution in the middle of the diaphragm is first extracted from the analysis. As stated earlier, hairpin bars have to be staggered to avoid space conflicts. Consequently, it is expected that the stresses resulting from the tensile force caused by the positive continuity moments to be asymmetric. Miller *et al.* (2004) suggested that the behavior of the detail is affected by the asymmetric stress distribution (e.g. crack widths varied). Fig. 7 represents two slices of the



(a) Normal stress in continuity diaphragm at center of 180-hook on left girder side

(b) Normal stress in continuity diaphragm at center of 180-hook on right girder side



(c) Top view of normal stress distribution in continuity diaphragm between girder ends

Fig. 7 Normal stress distribution at the bottom of the continuity diaphragm

continuity diaphragm defined by the projection of the girder's bottom flange on the diaphragm. The contours, which reflect the longitudinal normal stress intensity, confirm the expected asymmetric stress distribution. The difference between the two shown sliced sections is that one of them Fig. 7(a) is closer to one girder end, while the other is closer to the other girder end Fig. 7(b). It can be seen that the stress intensity in Fig. 7(a) is higher on the right side of the plot, while it is higher on the opposite side in Fig. 7(b). Fig. 7(c) is a top view of the same region; i.e., diaphragm between girders' bottom flanges. It can be seen that the tensile stresses flow from one girder end to the other while shifting the intensity to the side where the hairpin bars are biased as indicated by the shown arrows. This asymmetric stress distribution implies that assuming uniform behavior may underestimate the actual stresses in the design of the detail. While the difference caused by hairpin asymmetry may not be sufficient to initiate cracking, it may be exacerbated by other factors such as skewed layouts, thus leading to exceeding the tensile strength of concrete.

4.2 Hairpin bar contribution

Tensile forces are transferred between girder ends through the continuity diaphragm, where the hairpin bars serve as the main path for tensile forces from the girders to the diaphragm since the cold construction joint is not capable of resisting tensile stresses directly. When the joint is subjected to a positive moment, the girder-diaphragm interface breaks and a gap opens at the regions subjected to tensions (bottom), while regions subjected to compression remain intact. The developed model captured this behavior as can be seen in the scaled-up deformed shape shown in Fig. 8. At the gap, the entire tensile force is transferred thorough the only continuous element; i.e. hairpin bars. Fig. 9 shows a plot of the normal force in the hairpin bars. The spike in the axial force indicates the diaphragm-girder interface location where the gap takes place. The force in the hairpin bars start dropping away from the interface as it gets transferred to the diaphragm or girder concrete. Inside the diaphragm, the axial force diminishes just before the curved end of the 180°, whereas the tensile force changes to a compressive force inside the girder. The small compressive force inside the girder away from the diaphragm is the result of the prestressing force that increases until it reaches its full effective value at a distance equal to the transfer length.

4.3 Stress concentrations at girder ends

The previous section illustrates that the tensile force is almost solely transferred by the hairpin bars at the interface where the gap opens between the girder end and the continuity diaphragm. On either side of the interface, the girder or diaphragm concrete start contributing to the resistance of the tensile force gradually. Of interest to understanding the behavior of the continuity detail, the concrete stress distribution at the girders' ends is studied. Fig. 10 shows contours of the longitudinal normal stress, σ_x , across the girder section. The figures illustrate the higher stresses at the bottom flange and the lower stresses in the middle part of the section; i.e., web. This is especially true closer to the girder ends before more of the section starts getting engaged in the resistance of the tensile force according to St. Venant's principal. For example, the stresses at 2 inches from the girder end show that the maximum bottom flange normal stress exceeds the modulus of rupture for the girder concrete, which is determined to be around 1100 psi from laboratory testing. Conversely, stresses in the web hover around zero. At 32 inches from the girder end, the prestressing force is fully active and, therefore, compressive stresses are obtained in the bottom flange and the web. The gradual transition between these two sections can be seen in Fig. 10-b through e.

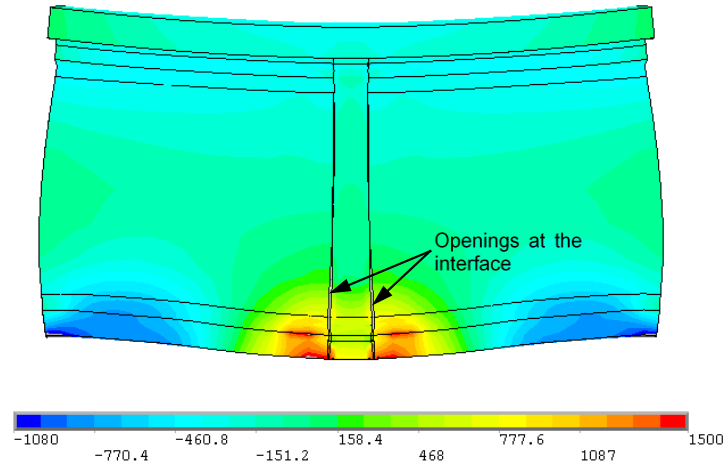


Fig. 8 Separation at the cold joint interface between girder ends and continuity diaphragm

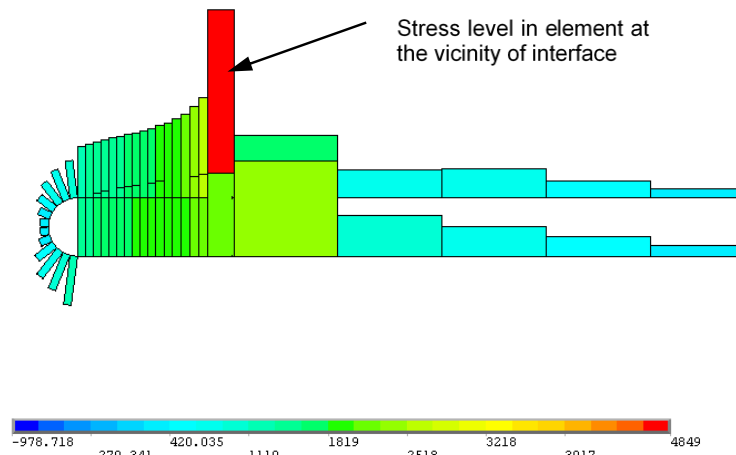


Fig. 9 Axial force distribution in a typical hairpin bar

It should be noted that in addition to these general observations about the stress distribution by girder parts; i.e., bottom flange and web, the stresses also show nonuniform distributions within each part. This is especially obvious closer to the girder ends where the analysis shows high tensile stresses at the top corner of the bottom flange. The monitoring system installed on this bridge segment did not call for sensors at this specific location. However, visual inspections revealed that one of the girders cracked at the same location where the FE analysis predicts high normal stresses. Fig. 11a and b show two pictures taken of the observed crack 6 months and 23 months after establishing continuity, respectively. It is clear from Fig. 11a that the crack initiated at the top corner of the bottom flange and did not extend all the way through the bottom flange. Seventeen months later, the crack propagated downward through the bottom flange. It should be noted that similar cracks were found in two other girders during a recent site visit. This indicates that the observed phenomenon is not an anomaly, but rather a behavioral attribute of the investigated continuity detail.

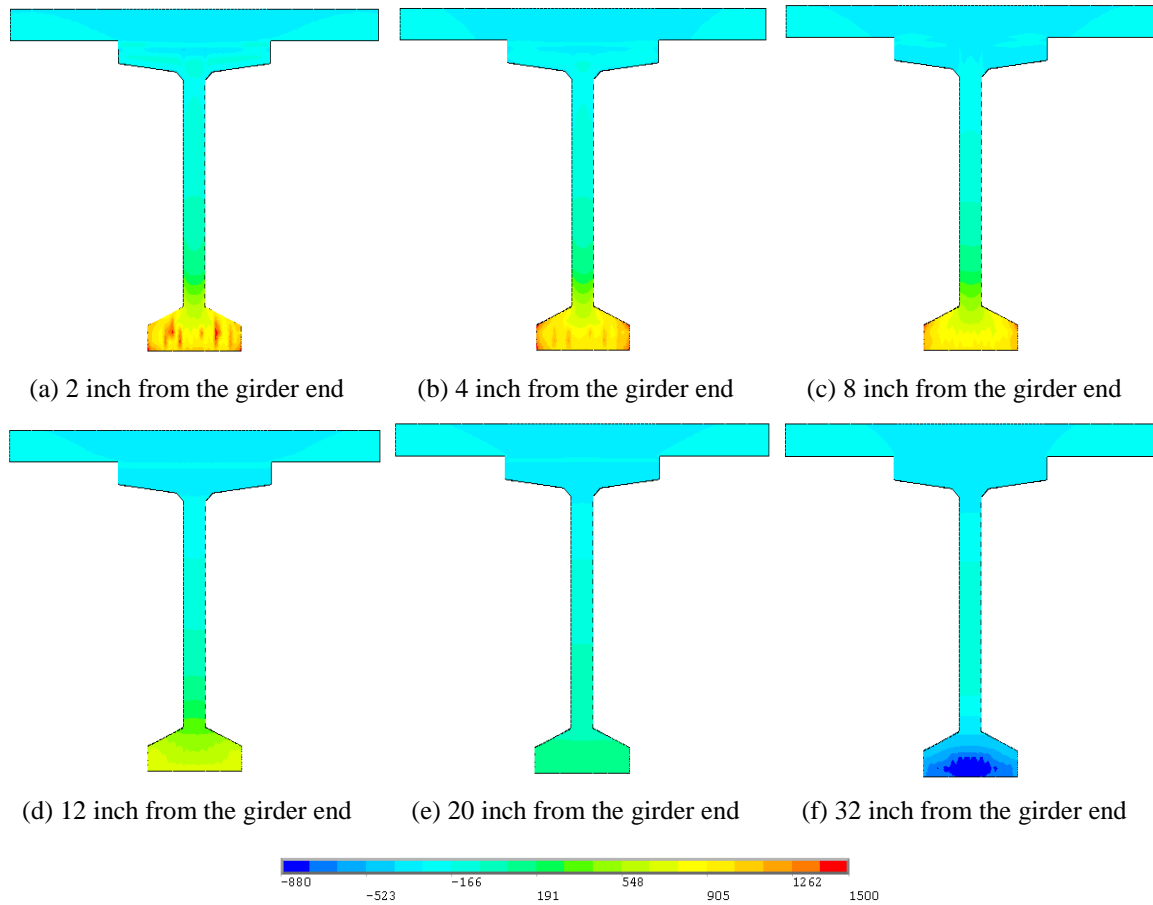


Fig. 10 Normal stress mapping at different locations of the composite section at girder ends

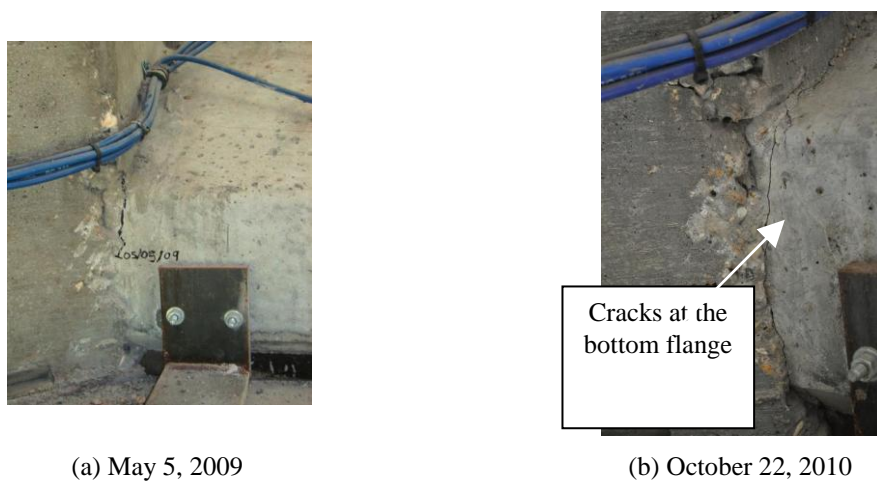


Fig. 11 Observed crack at the bottom flange of girder near the continuity diaphragm

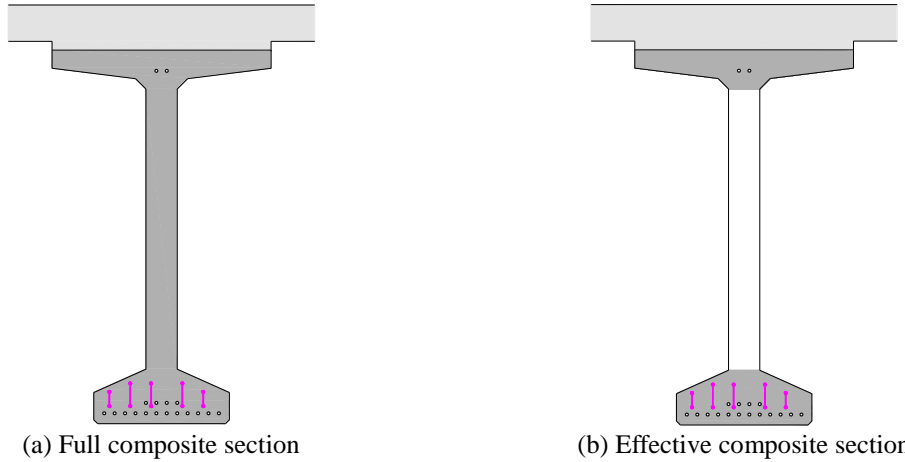


Fig. 12 Full and effective section geometry for calculation of moment of inertia at girder ends

5. Effective I_c for cracking moment calculations

In the previous section, it was illustrated that the entire girder section does not engage in resisting the tensile force close to girder ends. Thus, this continuity detail should be considered a disturbed region (Schlaich *et al.* 1987), which implies that the tensile force will be transferred through the concrete areas around the reinforcement only and not the entire section. Thus, checking the vulnerability of girder ends to cracking based on a cracking moment calculated according to the classical equations may lead to unconservative outcomes such as girder end cracking as was observed in the field. The cracking moment is normally checked using Eq. (2) (Nawy 2000):

$$M_{cr} = \frac{I_c}{y_b} \left[\frac{P_e}{A_{nc}} \left(1 + \frac{ec_b}{r^2} \right) + f_r \right] \quad (2)$$

where I_c is the composite section's moment of inertia, y_b is the distance from the extreme tension fibers to the center of gravity of the composite section, P_e is the effective prestress force after all the losses, A_{nc} is the area of the noncomposite girder section, r^2/c_b is the upper kern value of the noncomposite girder section, and f_r is the modulus of rupture of concrete, which was taken to be equal to $7.5\sqrt{f'_c}$, where f'_c is the compressive strength of concrete at 28 days in psi-units. It should be noted that additional terms accounting for dead loads on noncomposite section are not included in Eq. (2) as these moments are equal to zero at the support. It can be seen that the cracking moment, M_{cr} , is largely dependent on the effective prestress force and gross moment of inertia of the composite section. As stated earlier, the full effective prestress develops at a distance equal to the transfer length as seen in Fig. 3, which can be estimated using Eq. (1). Thus at the very end of the girder, the prestressing effect is negligible. Consequently, it can be said that the cracking moment is more influenced by the gross moment of inertia of the composite section as the first terms in Eq. (2) become small. Consequently, estimating I_c accurately is of even higher importance. The use of I_c assuming that the entire composite section is engaged in resisting stresses that develop from the positive moment will overestimate the cracking moment, M_{cr} . Therefore, it is proposed that an effective composite moment of inertia, I_{ce} , be used for cracking

moment calculations at girder ends.

The 3-D FE joint model has been used to identify the portion of the composite section that engages in resisting the normal stresses. Fig. 10 reveals that at small distances from the girder end (e.g. 2, 6 and 8 inches), the stress contours of the normal stresses are tension at the bottom flange only. Beyond 12 inches, stress concentrations start vanishing and a more uniform stress distribution takes place. Furthermore, the effective prestressing force increases away from the girder end, rendering the concern about cracking due to tension mute. Above the neutral axis, the deck concrete and the prestressed girder parts are subjected to compression and are fully engaged in the case of applied positive moment. Therefore, it is proposed that the effective gross moment of inertia be taken as that of the composite section after ignoring the web contribution for a distance equal to the transfer length measured from the girder end as can be seen in Fig. 12. For the Bulb-T (BT-72) composite section used in this study, the composite moment of inertia, I_c , is calculated to be 1,218,125 in⁴, whereas the proposed effective composite moment of inertia, I_{ce} , is only 968,349 in⁴. The difference between the two moments of inertia is 20.5%, which is how much current practice would overestimate the cracking moment for the proposed detail.

6. Conclusions

A 3-D detailed continuity joint model was developed using the commercially available software ANSYS to study the force transfer mechanism between girder ends in continuous prestressed concrete girder bridges. In the model, the actual geometry of 180° hook hairpin bars was precisely modeled as well as the cold joint that develops due to the construction at the interface between girder ends and the continuity diaphragms. Furthermore, the model accounts for the gradual transfer of the full effective prestress force at girder ends. The joint model was subjected to the service positive moments and shear forces simulating straining actions that would develop from time dependent creep effects. Based on results obtained using the detailed joint model, the following conclusions can be drawn:

1. The model revealed that due to the asymmetric configuration of the hairpin bars inside the continuity diaphragm, the normal stress distribution is also asymmetric which leads to stress concentrations.

2. At the cold joint interface, a gap develops between the girder ends and the continuity diaphragm under positive moment as the bond breaks between the two concretes; girders and continuity diaphragm. As a result, the tensile force is only transferred through the hairpin bars extending from the girder ends into the continuity diaphragm.

3. The existence of multiple causes of stress concentrations may lead to cracking if the cumulative stress exceeds the tensile strength of concrete, which was observed in the field and confirmed by the FE results.

4. The tensile force at the girder ends dissipates gradually away from the girder end confirming the St. Venant's principal. Furthermore, it was found that at the girder ends where the effect of prestress force is minimal, only the bottom flange, top flange and deck contribute in resisting stress.

5. It is proposed that the web portion of the girder be excluded from the composite moment of inertia calculation at girder ends for a length equal to the transfer length of the prestressing strands. This effective composite moment of inertia is proposed to address the lack of girder's web contribution to resisting the positive moment.

Acknowledgment

This research is sponsored in part by the Louisiana Transportation Research Center under Project # 08-1ST. Additional support from the Department of Civil and Environmental Engineering at Louisiana State University was received. Any opinions, findings, and conclusions or recommendations expressed in this material are those of the authors and do not necessarily reflect the views of the sponsoring agencies. The authors would like to thank Mr. Walid Alaywan, P.E. (LTRC), Mr. Hossein Ghara, P.E. and Mr. Paul Fossier, P.E (LA-DOTD) for their invaluable input and support to this project.

References

- AASHTO (2010), *LRFD Bridge Design Specifications*, American Association of State Highway and Transportation Officials, Washington, D.C.
- ANSYS (2008), *Theory Reference*, ANSYS, Inc., Canonsburg, PA.
- Caner, A., Dogan, E. and Zia, P. (Mar. 2002), "Seismic performance of multisimple-span bridges retrofitted with link slabs", *J. Bridge Eng.*, ASCE, **7**(2), 85-93.
- Caner, A. and Zia, P. (1998), "Behavior and design of link slabs for jointless bridge decks", *PCI J.*, Precast/Prestressed Concrete Institute, **43**(3), 68-80.
- El-Safty, A. and Okeil, A.M. (2008), "Extending the service life of bridges using continuous decks", *PCI J.*, Precast/Prestressed Concrete Institute, **53**(6), 96-111.
- Hastak, M., Mirmiran, A., Miller, R.A., Shah, R. and Castrodale, R. (2003), "State of practice for positive moment connections in prestressed concrete girders made continuous", *J. Bridge Eng.*, **8**(5), 267-272.
- Hossain, T., Okeil, A.M. and Cai, C.S. (2013a), "Calibrated finite element modeling of creep behavior of prestressed concrete bridge girders", (*Accepted for publication in ACI Struct. J.*).
- Hossain, T., Okeil, A.M. and Cai, C.S. (2013b), "Field test and finite element modeling of a three span continuous girder bridge", *J. Perform. Constr.Facil.*, ASCE, **28**(1), 136-148.
- Hossain, T., Segura, S. and Okeil, A.M. (2012), "Analytical and field measured temperature profile and its structural effects on a continuous girder bridge", (*submitted for publication in the ASCE J. of Bridge Engineering*).
- Kim, T.H., Cheon, J.H. and Shin, H.M. (2012), "Evaluation of behavior and strength of Prestressed Concrete Deep Beams Using Nonlinear Analysis", *Comput. Concrete*, **9**(1), 63-79.
- Lee, D.H., Hwang, J.H., Ju, H. and Kim, K.S. (2014), "Application of direct tension force transfer model with modified fixed-angle softened-truss model to finite element analysis of steel fiber-reinforced concrete members subjected to shear", *Comput. Concrete*, **13**(1), 49-70.
- Miller, R.A., Castrodale, R., Mirmiran, A. and Hastak, M. (2004), *Connection of Simple-Span Precast Concrete Girders for Continuity*, NCHRP Report 519, Transportation Research Board, Washington, D.C.,
- Mirmiran, A., Kulkarni, S., Castrodale, R., Miller, R. and Hastak, M. (2001), "Nonlinear continuity analysis of precast, prestressed concrete girders with cast-in-place decks and diaphragms", *PCI J.*, Precast/Prestressed Concrete Institute, **46**(5), 60-80.
- Nawy, E.G. (2000), *Prestressed Concrete A Fundamental Approach*.
- Newhouse, C.D., Roberts-Wollmann, C.L., Cousins, T.E. and Davis, R.T. (2008), "Modeling early-age bridge restraint moments: creep, shrinkage, and temperature effects", *J. Bridge Eng.*, **13**(5), 431-438.
- Oesterle, R.G., Glikin, J.D. and Larson, S.C. (Jan. 1989), *Design of Precast Prestressed Bridge Girders Made Continuous*, NCHRP Report No. 322, Transportation Research Board, Washington, D.C.,
- Okeil, A.M. and El-Safty, A.K. (Nov. 2005), "Partial continuity in bridge girders with jointless decks", *Pract. Period. Struct. Des. Constr.*, ASCE, **10**(4), 229-238.
- Okeil, A.M., Cai, C.S., Chebole, V. and Hossain, T. (2011), "Evaluation of continuity detail for precast

- prestressed girders”, 477, Louisiana Transportation Research Center, Baton Rouge, LA, p. 198.
- Okeil, A.M., Hossain, T. and Cai, C.S. (2013), “Field monitoring of positive moment continuity detail in a skewed prestressed concrete bulb-T girder bridge”, *PCI Journal*, Precast/Prestressed Concrete Institute, **SPR 2013**, 2-12.
- Peterman, R.J. and Ramirez, J.A. (1998), “Restraint moments in bridges with full-span prestressed concrete form panels”, *PCI Journal*, Precast/Prestressed Concrete Institute, **43**(1), 54-73.
- Salmons, J.R. and May, G.W. (1974), *Strand Reinforcing for End Connection of Pretensioned I-Beam Bridges, Interim Report 73-5B*, Missouri Cooperative Highway Research Program, Missouri State Highway Department.
- Schlaich, J., Schäfer, K. and Jennewein, M. (1987), “Toward a consistent design of structural concrete”, *PCI J.*, Precast/Prestressed Concrete Institute, **32**(3), 74-150.
- Shang, F., An, X.H., Kawai, S. and Mishima, T. (2010), “Open-slip coupled model for simulating three-dimensional bond behavior of reinforcing bars in concrete”, *Comput. Concrete*, **7**(5), 403-419.
- Shayanfar, M.A. and Safiey, A. (2008), “A new approach for nonlinear finite element analysis of Reinforced concrete structures with corroded reinforcements”, *Comput. Concrete*, **5**(2), 155-174.
- Sousa, C., Sousa, H., Neves, A.S. and Figueiras, J. (2012), “Numerical evaluation of the long-term behavior of precast continuous bridge decks”, *J. Bridge Eng.*, **17**(1), 89-96.
- Timoshenko, S.P. and Gere, J.M. (2009), *Theory of Elastic Stability*, Dover Publications, USA.
- Wang, W.W., Dai, J.G., Huang, C.K. and Bao, Q.H. (2011), “Strengthening multiple span simply-supported girder bridges using post-tensioned negative moment connection technique”, *Eng. Struct.*, **33**(2), 663-673.